Co-published by
**Institute of Fluid-Flow Machinery**
Polish Academy of Sciences
**Committee on Thermodynamics and Combustion**
Polish Academy of Sciences



http://www.imp.gda.pl/archives-of-thermodynamics/

# Heat transfer enhancement by drop impact onto a nanotextured superheated surface

Ravi Pippal[a], Aditi Agrawal[a], Akshita[a], Tulip Biswas[a], Deepali[a], Pushpendra Kumar Shukla[a], Sumit Sinha-Ray[a,b*]

[a]Department of Textile and Fibre Engineering, Indian Institute of Technology - Delhi, Hauz Khas, New Delhi 110016, India
[b]Department of Mechanical and Industrial Engineering, University of Illinois at Chicago, Chicago, IL 60607-7022, USA
*Corresponding author email: ssinharay@textile.iitd.ac.in

Received: 22.05.2025; revised: 30.01.2026; accepted: 11.02.2026

## Abstract

Thermal management of microelectronics has become a major concern for the semiconductor industry, especially for high-power applications, due to the requirements of large computations in a smaller packing. Here in this work, spray/drop impact cooling of microelectronics (hot spot cooling) is studied, using a heat sink with novel nanotexture on the surface. The adherent nanotexture with highly porous architecture was fabricated with polymeric nanofibres obtained from supersonic solution blowing. The impacting drops on the superheated bare surface visibly bounced and escaped, exhibiting a Leidenfrost phenomenon, whereas, for the coated surface, complete suppression of the Leidenfrost effect was observed. For a nanotextured surface, the impacting droplet was focused hydrodynamically to penetrate the porous layer and wick through the network, thereby getting pinned, despite the fibrous architecture being hydrophobic. The overall heat transfer rate was measured to be in excess of 1000 kW/m$^2$ from the coated surface, as calculated from the wetting area. Later, it was also found that a drop interval time of 2.5 s yielded the optimised cooling for both short- and long-time applications. The long-time heating and cooling cycles exhibited a repeatable cooling pattern between the upper critical (130$^o$C) and lower safe (80$^o$C) range, demonstrating the excellent robustness of the nanofibrous texture and a possible route of preservation of coolant.

**Keywords:** Drop impact cooling; Nanofibre; Nanotextured surface; Thermal management; Leidenfrost phenomenon.

Vol. 47(2026), No. 1, 101–111; doi: 10.24425/ather.2025.156858

Cite this manuscript as: Pippal, R., Agarwal, A., Akshita, Biswas, T., Deepali, Shukla, P.K., & Sinha-Ray, S. (2026). Heat transfer enhancement by drop impact onto a nanotextured superheated surface. *Archives of Thermodynamics*, 47(1), 101−111.

## 1. Introduction

The advent of electronic computers in the 1940s initiated a significant industrial transformation, focusing on the creation of faster and more efficient calculations [1]. With the progress of mankind, yielding the need for large data computation, a notable shift in integrated circuit designs resulted in significant enhancements in processing speed within a strict geometric confinement. Consequently, the thermal loads on these devices have increased considerably. Modern electronic devices now generate a substantial heat flux (~200 W), while most such microelectronic devices fail beyond their operating temperatures of 75−80$^o$C [2]. According to a report by Industrial Credit and Investment Corporation of India (ICICI) Direct, India's electronic manufacturing sector is expected to experience significant growth, expanding from USD 12 billion to USD 250 billion within the next five years [3], out of which thermal management of electronic packages will constitute a major part.

The current requirement of heat removal from microelectronic chips can be as high as 1 MW/m$^2$. Efficient cooling systems are required to manage this heat, with heat transfer coefficients (HTC) ranging from 10 to 30 kW/(m$^2$·K) to maintain safe operating temperatures [4]. This cannot be achieved via air cooling, since HTC of forced air can only be as high as

## Nomenclature

$C$ – specific heat, J/(kg·K)
$g$ – gravitational acceleration, m$^2$/s
$h$ – convective heat transfer coefficient, W/(m$^2$·K)
$k$ – thermal conductivity, W/(m·K)
$p$ – pressure, kPa
Pr – Prandtl number
Re – Reynolds number, Re = $Dv\rho\ /\mu$
$t$ – time, s
$T$ – temperature, K
$U$ – hydrodynamic focusing velocity, m/s
$V$ – impregnation velocity, m/s

### Greek symbols

$\alpha$ – thermal diffusivity, m$^2$/s
$\mu$ – dynamic viscosity, Pa·s
$\rho$ – density, kg/m$^3$
$\sigma$ – surface tension, N/m

### Subscripts and Superscripts

$\infty$ – atmospheric
*eff* – effective
*pore* – pore of textured surface

### Abbreviations and Acronyms

CPU – central processing unit
DMF – dimethylformamide
HTC – heat transfer coefficient
PAN – polyacrylonitrile
PCL – polycaprolactone
PTFE– polytetrafluoroethylene
PVDF– poly-vinylidene fluoride

5−20 W/(m$^2$·K). Hence, air cooling is not a viable solution for future computing techniques, which also poses a significant environmental hazard in terms of total carbon emissions.

To mitigate these issues, microelectronics cooling techniques are intensified with direct cooling techniques. Direct cooling methods include approaches such as spray and jet impingement cooling, boiling, immersion cooling, drop impact and droplet electrowetting [5–9], etc. Although methods like boiling, immersion, etc. are highly efficient and can potentially remove the desired quantity of heat (~1 MW/m$^2$), the rationale for choosing liquid drop impact (a type of flash evaporative technique) is to minimise the size of cooling components and concentrate cooling efforts where they are most needed. By focusing on the primary heat source, the central processing unit (CPU), the cooling system's size and complexity can be reduced [10]. Other components, such as the random access memory (RAM), hard drives, fans and the motherboard, typically generate less heat. Thus, effective cooling of CPU can significantly reduce the overall thermal load. The significant cooling potential of drop impact is linked to the evaporation of liquid at the hot surface. The efficiency of this process is greatly influenced by the hydrodynamics and heat transfer associated with drop impact on hot surfaces. However, the usual receding motion of the spread-out liquid lamellae on superheated metal surfaces often results in complete drop bouncing, interrupting the cooling process. Additionally, the insulating vapour layer that forms between the drop and the surface significantly reduces the heat flux, generating a Leidenfrost-like effect.

Surfaces, modified to become wettable [11] or rendered porous/textured [12], can often lead to minimisation of the Leidenfrost phenomenon and can improve heat transfer. In various cases, such surface modification techniques are not cost-effective and scalable. A novel method of surface modification involves coating of superheated surfaces with non-woven polymer nanofibre mats [13,14], which are highly porous, and can enhance wettability effects or reduce surface energy [15]. The advantages of using nanofibre mats in flash evaporative cooling, like drop impact cooling, primarily stem from their impact on the hydrodynamic behaviour of the impacting drops and the increased heat transfer area. Previous studies have identified two key features of drop impact on nanofibre mats [14]. Firstly, receding, splashing and bouncing during the impact on polymer nanofibre mats are almost eliminated. The drop spreads similarly to an impermeable surface, but the contact line gets pinned at the maximum spread diameter, which prohibits receding. Secondly, drop spreading is accompanied by the impregnation of pores, which takes place almost instantaneously. This enables the liquid to wick inside the nanofibre mat over a substantially wider area than that enclosed by the fixed contact line. Both features enhance heat transfer by enlarging the contact area between water and the underlying hot surface [5].

This research delves into the outcome of drop spreading on and within nanofibre mats. The primary focus is to investigate the effects of liquid drop impact on a nanofibrous textured surface and the associated temperature distribution, along with the fate of the impacting drop and superheated substrate. This is examined under various conditions – different frequencies of drop impact and cycles of test conditions.

## 2. Literature review and objectives

Drop impact on superheated substrate is a well-researched topic. This domain of study is often considered under spray cooling techniques. Voluminous research data are available to address the hydrodynamic behaviour of an impacting drop, which is often governed by the impact parameters like impact velocity, impacting drop diameter/mass, liquid's thermophysical properties, surface texture and wettability [16].

Along with experimentation studies of impacting drop-surface interaction with variable surface or process parameters [17,18], several computational approaches have also been utilised, like molecular dynamic simulation [19], Lattice-Boltzmann method [20], volume of fluid method [21], or a more recent approach of phase-field modelling [22]. Out of these computational approaches, the phase-field method has gained immense popularity due to its robustness in droplet impact/interaction-based studies on a solid medium [23,24].

Despite the recent advances, one of the concerning aspects of drop impact on surfaces is the non-isothermal case, where the surface superheat is to be considered along with several other phase-change heat transfer regimes like nucleate boiling, transition boiling, atomisation and film boiling (Leidenfrost phe-

nomenon), and natural convection affecting sensible heat. Several studies have focused on microstructural surfaces like micropillar [25,26], mesh [27], sputtered network [28], and many more, to understand the phase change at the pinning sites of impacting liquid droplets and their behaviour during film boiling conditions. Especially, such studies have focused intensively on variable wettability and varying roughness.

For the sake of brevity, this literature review specifically focuses on nanotextured surfaces having a 'furry coat' like architecture, derived from a polymeric fibrous network and surface-impacting drop interaction at atomisation and film boiling conditions. One of the earliest studies of drop impact on fibrous structure was conducted by Srikar et al. [13], which demonstrated the phenomenon of hydrodynamic focusing of droplets onto electrospun nanofibrous textured surfaces, aiding liquid penetration into the net-like structures and enhancing wicking, while preventing liquid receding and bouncing. Further, it was shown that such a nanofibrous structure, due to the spontaneous wicking at a specific impacting velocity, could potentially reverse the Leidenfrost effect [29]. These nanofibrous membranes after copper plating revealed a 'thorny-devil' like architecture having nanoscale roughness on individual fibres. This process enhanced hydrophilicity and increased heat transfer from superheated surfaces. Potentially such a surface could remove heat at the rate of ~10MW/m$^2$ [30]. In all these cases, it was observed that the liquid penetration velocity within the pores can be significantly higher than the Washburn velocity (wettability), or the Tanner velocity (spreading), since a large amount of kinetic energy of an impacting drop can be channelised through the interconnected pores of the nanotextured surfaces. This focusing velocity is by 2−3 orders of magnitude higher than the impacting liquid drop velocity [14]. This makes the hydrodynamic focusing possible even on superhydrophobic porous surfaces. Sahu et al. [8] studied the impact of polar (water) and non-polar liquid (Fluorinert FC7500, hexane) drops onto electrospun nanofibre membranes made of varying degrees of wettability, with polymers like: PAN (polyacrylonitrile), nylon, PCL (polycaprolactone) and teflon. It was observed that liquid penetration occurred at velocities of 1.5−3 m/s, regardless of surface hydrophobicity, with less wettable membranes requiring higher threshold velocities. Liquids with lower surface tension penetrated more easily, mimicking a millipede-like jet system, whereas high surface tension liquids, like water, pass through a thin electrospun membrane like a jet. Even superhydrophobic teflon membranes could not prevent water penetration at high-impact velocities, especially at thinner dimensions (<100 μm).

Although the study emphasised an important breakthrough in terms of dynamic penetration of liquids, long-term degradation of nanofibre coatings remained a potential concern, especially under mechanical stress and repeated impacts. The same was discussed by Sahu et al. [31], who examined the penetration of aqueous nanofluid drops into non-wettable porous membranes through hydrodynamic focusing. This phenomenon enabled liquid penetration into materials like PTFE (polytetrafluoroethylene), which typically repel water. The study compared a wettable porous surface (glass fibre) and a non-wettable membrane (PTFE), highlighting the dominance of drop impact dynamics over wettability.

Sinha-Ray and Yarin [32] investigated the heat transfer enhancement of nanotextured surfaces during droplet cooling using water and Fluorinert FC-7300. Smaller droplets of water at higher frequencies, especially at 4 Hz, resulted in maximum heat flux removal of 0.9 MW/m$^2$, balancing coolant supply and evaporation. The study emphasised the previously discussed conditions and showed the importance of dynamic focusing of liquid droplets and wicking into the nanotextured porous surface. A similar behaviour was seen even in zero-g conditions as well [33]. However, both studies were limited to short-term effects and lacked insights into long-term surface degradation, if any. A very recent study conducted by Park et al. [5] demonstrated a significant improvement in thermal management of microelectronics components using electrospun/supersonically sprayed/electrodeposited thorny-devil-like nanofibrous/nanowire architecture and reported a maximum 56% enhancement in effective heat transfer coefficient [5]. They also reported heat flux removal as high as 1.1−2 MW/m$^2$ from the metal nanowire textured surface. Although all these studies elucidated the numerous benefits of nanofibrous architecture, it is needless to mention that the above-mentioned articles utilised metal-plated surfaces, which are cost-ineffective, requiring significant sophistication and lacking in scalability and generalisability. At the same time, electrospun polymeric fibrous layers are highly fluffy in nature, and they can only be deposited on limited geometries, while facing significant threats of delamination during any vigorous heat transfer studies.

A greater need is therefore required to understand the effect of pure polymeric nanofibrous coating on heat removal from microelectronics cooling and/or a significant reduction of surface superheat. It has been previously discussed in Refs. [34–37] that a pure polymeric nanofibrous network deposited by supersonic solution blowing exhibited a robust behaviour under vigorous boiling regime, whereas in the work of Jun et al. [6], a possible delamination of metal-plated fluffy electrospun layers was discussed. The supersonically blown nanofibres were reported to be instrumental in boiling heat transfer, as they could potentially withstand several hours of rigorous heat transfer processes [38], and reduce significant surface superheat. This begs an important question – can such an ultrafine polymeric surface withstand a flash evaporation of an impacting liquid drop when the surface is under superheated conditions? All the previous articles concerning drop impact and associated heat transfer studies on polymeric/polymeric-metal coated surfaces have been related to wettable/semi-wettable surfaces, with fluffy architecture, where a coating thickness of ~50−100 μm was considered [5,13,29]. However, none of these articles resorted to a long-time or cyclic test pattern. Hence, in this article, the authors reported an investigative study on drop impact heat transfer of water on a hydrophobic and thin (~ 10 μm) polymeric architecture, which was deposited on a superheated copper substrate. The substrate mimicked an electronic surface exposed to extreme conditions (>120°C) for compact integrated circuits. To the best of the authors' knowledge, such a study is rarely available, which elaborately discusses the drop impact heat transfer on a thin hydrophobic polymeric fibrous coated superheated surface and tests

its robustness in a long-term study. Our hypothesis is that the impacting velocity of the droplet would surpass the wettability effects due to hydrodynamic focusing and would still allow the droplet to spread and evaporate without allowing the Leidenfrost effect, even in such thin coating. Eventually, the said layer is expected to be robust and effective in evaporative cooling.

## 3. Materials and methods

### 3.1. Materials

Poly-vinylidene fluoride (PVDF) was acquired from Thermo Fisher Scientific (Alfa Aesar). Dimethylformamide (DMF) was acquired from Alfa Aesar. Acetone was purchased from Thermo Fisher Scientific. Copper and teflon were sourced from the local suppliers in Delhi. Thermal paste (MX-4 thermal compound) was also purchased locally. A thermometer (USB TC08) and K-type thermocouples were obtained from Omega. Cartridge heaters (50 W each) were sourced from Watlow.

### 3.2. Coating of nanofibres on copper block via supersonic solution blowing

The schematic of the experimental set-up is shown in Fig. 1.

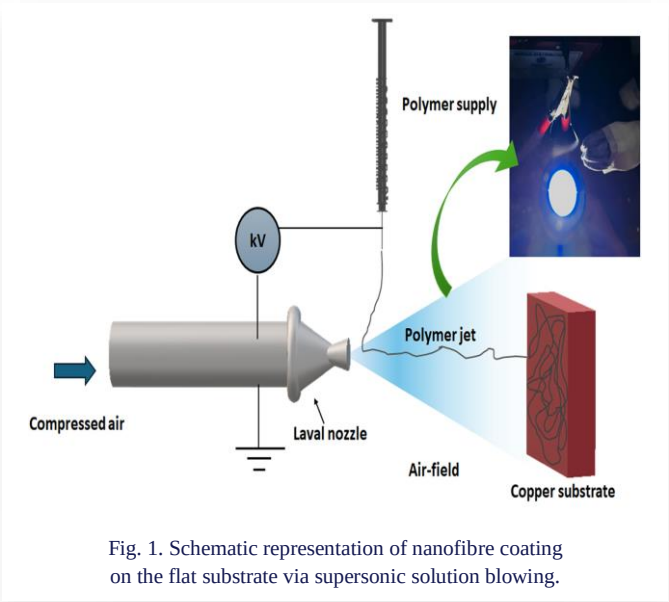


Fig. 1. Schematic representation of nanofibre coating on the flat substrate via supersonic solution blowing.

For supersonic solution blowing, an 8 % wt. PVDF solution was prepared in dimethylformamide (DMF) and acetone in a 1:1 ratio. The polymer solution was kept on a hot plate magnetic stirrer at 60°C and 600 rpm overnight to ensure homogeneous mixing and dissolution. The prepared polymer solution was loaded into a 5 ml syringe and pumped through a 22G needle at a flow rate of 0.7 ml/hr with the use of a syringe pump (New Era Pump System Inc.). A compressor, operating at 150 psi (≈10,34 bar), was linked to a supersonic de Laval nozzle (Silvent 209 L). The needle tip, dispensing the polymer solution, and the gas nozzle exit were positioned 1.5 cm and 1cm apart in horizontal and vertical directions, respectively. The nozzle was grounded, while a 6.5 kV electric potential was supplied to the needle tip. The nanofibres were collected on a copper block positioned 25 cm from the nozzle exit. The nanofibres were deposited on a copper substrate for a duration of 3 minutes to have a milky appearance on the copper block of dimensions 25 mm (length) × 12.5 mm (width) × 5 mm (thickness).

### 3.3. Characterisation

Following the coating process, the fibrous architecture was analysed using scanning electron microscopy (SEM) (ZEISS EVO 50), and the contact angles of bare and nanotextured surfaces were measured using a goniometer (Data Physics OCA 15LJ). The SEM images exhibited a highly porous architecture with a mean fibre diameter of 244 nm with a standard deviation of 63 nm. Contact angle measurements revealed that the bare copper surface was wetted by water droplets, having a contact angle of 77°, Fig. 2C(a), indicating hydrophilic behaviour. This is likely attributed to the presence of oxide layers on the copper substrate. In contrast, the nanofibrous nanotextured surface substrate exhibited a contact angle of approx. 137°, Fig. 2C(b), demonstrating a hydrophobic modification of the surface.

### 3.4. Experimental setup

The schematic of the drop impact setup is shown in Fig. 2 (both schematic and the actual image). The components of the experimental setup are as follows:

- Primary components: (a) copper substrate, (b) teflon block, (c) auto-transformer connected to (d) two cartridge heaters, placed into the copper block to supply uniform heat, (e) 24G bent needle connected to (f) syringe pump to supply the liquid to the heated surface, (g) thermometer, and (h) two thermocouples,
- Secondary components: (i) high-speed camera, (j) light source, (k) computer.

The copper substrate was placed onto the heated copper block of similar dimensions, where the heated block acted as the heat source, powered by two cartridge heaters (3 mm in diameter and 25 mm in length), operating at a certain voltage, and the copper substrate was the sink, which was subjected to drop impact. A thin layer of thermal paste was applied between these two copper blocks to eliminate any air gap. The whole assembly was affixed within a groove of teflon to resist heat loss from the sides, and only the top surface of the heat sink was exposed to the environment. Two holes having a diameter of 1.5 mm were drilled up to the centre of the upper copper substrate, 2 mm from the top surface. This was done to understand the surface temperature. The distance between the thermocouples was 1 cm, and every time the liquid was dropped between these two thermocouples to read an average temperature of the surface. These thermocouples were read as $T_1$ and $T_2$. Since copper has a very high thermal diffusivity (~$10^{-4}$ $m^2/s$), the thermal transient time between the upper surface and the thermocouple locations would be ($L^2/\alpha$) < 40 ms, and hence, a steady thermal gradient would prevail. Consequently, for a measured temperature of 125°C and room temperature of 25°C with the heat transfer coefficient of still air as 5 W/($m^2$·K), the heat loss from the surface could be estimated as $Q_{loss} = h \cdot A \cdot \Delta T$, yielding a value of 0.15 W. This value was much smaller compared to the overall heat supply mentioned in the latter section, and hence, the thermocouples allowed an accurate estimate of the surface temperature.

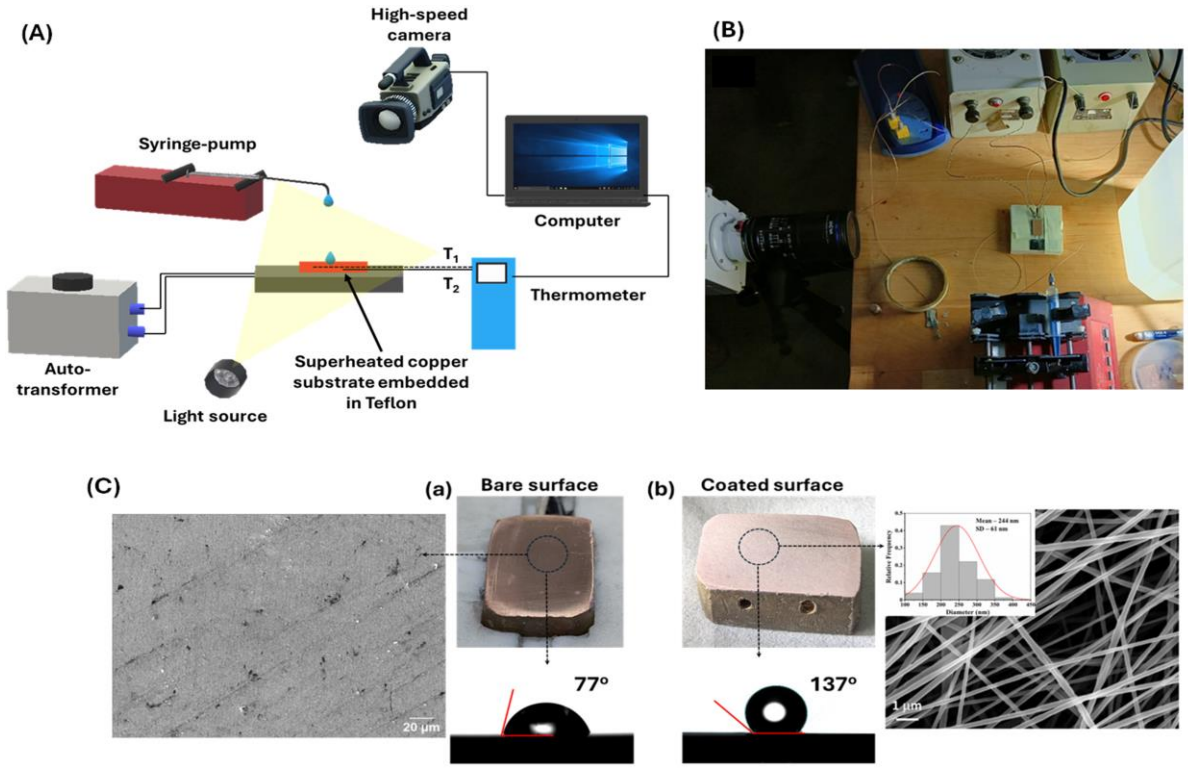


Fig. 2. (A) Graphical representation of the test scheme; (B) an actual photograph of the experimental setup; (C) the real image of the copper substrate, and its SEM image and contact angle measurement, followed by a fibre coated surface having a milky white appearance along with the SEM image of the fibrous network and fibre size distribution.

A high-speed camera, connected to a computer, was employed to capture the dynamics of water droplets impacting both the bare and nanotextured superheated surfaces.

### 3.5. Drop impact experiment

First, the copper substrate was smoothened using 1000, 1200 and 2500 grit sandpaper, in s sequential manner to obtain a mirror finish. Once the setup was assembled, two K-type thermocouples ($T_1$ and $T_2$, accuracy of ±1°C) were inserted into the copper substrate and connected (by USB TC08) to a thermometer (refer to Fig. 2 for locations of $T_1$ and $T_2$). The thermometer was then connected to a PC to record temperature readings. Two separate variable autotransformers provided electric power to the cartridge heater assembly. Throughout the trials, the supply voltage was maintained at a specific value, resulting in an overall supply of power 40 W ($P = V{\cdot}I$, $V$ – voltage, $I$ – current) or heat flux of 128 kW/m$^2$. When the temperatures ($T_1$ and $T_2$) reached 125°C, water droplets were introduced onto the superheated surface. The voltage supply to the heaters was cut off when the temperatures ($T_1$ and $T_2$) reached 140°C or above, and the experiments were stopped. This is later called a dry-out situation in later sections. In a separate scenario, the drop impact was halted again, when the temperatures ($T_1$ and $T_2$) came close to 105−110°C, when a liquid puddle started to form. This is indicated as a flooding regime in later sections. Experiments were conducted at various drop impact rates of water to ascertain the critical and optimised droplet frequency. The optimisation ensured a steady surface temperature, while preserving the coolant. Here, a steady temperature can be visualised as constant working of high-power microelectronics, without overheating. Temperature readings were recorded and analysed using logging software to gain insights into heat transfer dynamics under these optimised conditions. A high-speed camera was employed to capture droplet dynamics such as receding, splashing, bouncing and spreading. Separately, the experiments were conducted to obtain the optimum flow rate to distinguish between bare and nanotextured surfaces. Surface robustness was also evaluated at the optimised flow rates to ensure sufficient heat removal, while not allowing the surface to go beyond a specific upper limit. During such tests, the heat supply was not cut off, mimicking a consistent microelectronics performance throughout.

### 3.6. Drop size evolution during impact

To capture the dynamic behaviour of the water droplet during impact and atomisation, a high-speed imaging system (Phantom VEO 1310L) was employed. The camera view was set at a resolution of 640×360 pixels, with a sampling rate of 10000 fps, and an exposure of 50 µs to ensure precise spatial resolution. The initial radius of the droplet was used as the calibration, precisely measured from its mass and thereafter converted to volume, using the density of 1000 kg/m$^3$ (at room temperature). The oncoming droplet can be observed in the first frame in Fig. 3. The droplet radius was measured to be 0.142 cm (for a droplet mass of 11.9 mg), corresponding to an estimated volume of 0.012 cm$^3$. All the successive image analyses were done using the above-mentioned calibration and ImageJ software. A total of 700 individual frames from an entire video were analysed for a single droplet impact-bouncing-atomisation event. The gap

between the two analysing frames was 150, capturing the entire droplet life cycle till it left the heater surface. The frame gap of 150 was rationally chosen to avoid in calculations any satellite droplets generated during atomisation. This helped to reduce the overestimation of satellite droplet counting. The visualisation area (in pixels) was converted to physical units (cm or $cm^3$), approximating a spherical contour.

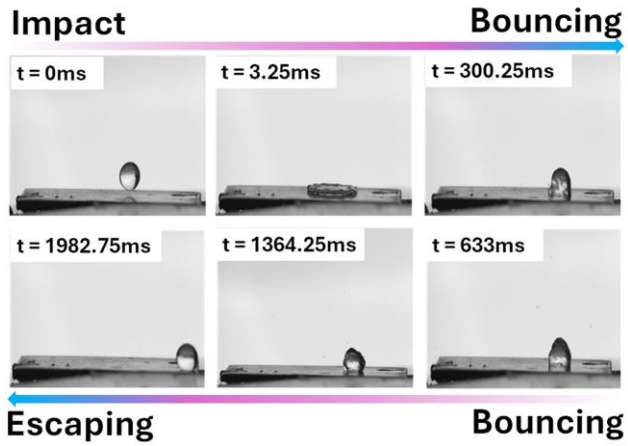


Fig. 3. Snapshots from high-speed imaging of a water droplet impacting on the superheated bare substrate, which reflect a complete impact-spread-bounce-escape pattern.

### 3.7. Uncertainty of measurements

The maximum estimated uncertainty of heat flux was measured to be [39]:

$$\frac{\Delta(Q/A)}{(Q/A)} = \sqrt{\left(\frac{\Delta I}{I}\right)^2 + \left(\frac{\Delta V}{V}\right)^2}.$$

As per the manufacturer, the voltage uncertainty was ±2%, and the uncertainty in current was ±10 mA. This led to an overall error of 2.24% in heat flux measurements, i.e. an error of ±5.12 $kW/m^2$.

## 4. Results and discussion

The experiments were initially focused on understanding the water droplet behaviour on the superheated surface, after it made an impact. A high-speed camera was configured to capture the complete impact, receding, bouncing, spreading and atomisation behaviour, at 4000 fps. During the tests, it was observed that on a bare surface, the liquid drop exhibited a bouncing and escaping pattern, a phenomenon akin to the Leidenfrost effect. The liquid droplet of mass 11.9 mg (radius 0.142 cm) was released from a height of 30 cm, indicating an impact velocity of nearly 2.42 m/s. At this velocity, the Weber number ($We = \rho u^2 d/\sigma$, with $\rho$ as the liquid density, $u$ as the impacting velocity, $d$ as the drop diameter and $\sigma$ as the surface tension) could be calculated as 124.45, which signifies an inertia driven phenomenon surpassing the surface tension. This would invariably lead to an imminent liquid rebound with complete splashing below 5 ms. Figure 3 shows the impacting drop behaviour on the superheated bare surface with the surface temperature of 125°C.

The images in Fig. 3 show the life cycle of the droplet and its interaction with the superheated surface, where a small change in the droplet's actual size is self-explanatory. It clearly shows that the impacting drop stayed on the surface for nearly 2 s before escaping the surface completely. This happened due to the rapid evaporation at the contact line, almost like film boiling, helping to create a vapour cushion, which levitated the drop from the superheated surface. A more detailed visualisation, with an illumination corrected image, is shown in Fig. 4.

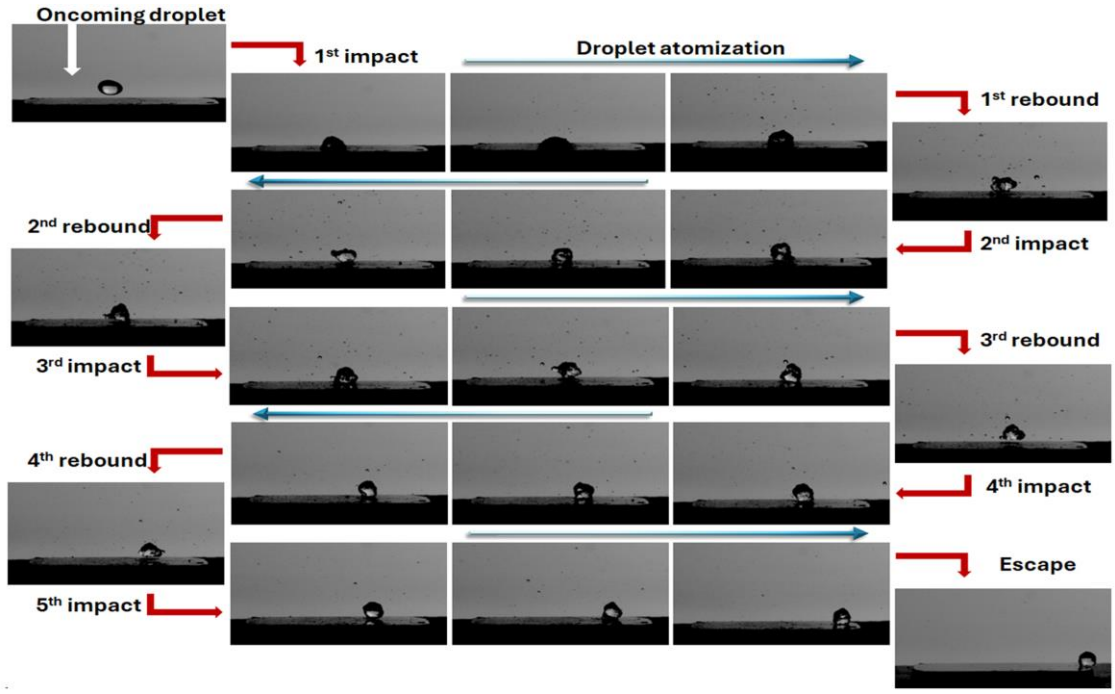


Fig. 4. Snapshots from high-speed imaging of a water droplet impacting on the superheated bare substrate, which shows different stages of impact, atomisation, rebounding and escape patterns.

A close-up view of the same impacting droplet, recorded at a higher speed (10000 fps) helped observe the entire impact, rebound and escape route, along with atomisation. This is commonly observed in film boiling like situations, which were enhanced due to inertial effects during impact. Five stages of impact-bouncing-escaping and atomisation are shown in the figures, and one can easily find the small droplets escaping from a parent droplet and the viewing window. The departing droplet was calculated to have a radius of 0.13 cm, as measured from image analysis, with a calculated volume of 0.0092 $cm^3$ or mass of 9.2 mg. This suggested a 61.35% of mass escaping due to the Leidenfrost effect. A careful calculation from image analysis, using the routine mentioned in Section 3.6, shows that about 30% of mass was lost due to fragmentation or atomisation. The remaining mass loss could be accounted for (a) insignificant evaporation during impact stages, leading to almost no temperature change of the surface, (b) minor error in calculations in droplet sizes arising during pixel to physical unit conversion, or (c) inaccuracy of droplet count due to ultra-small size in the narrow depth of the field. The error could also come from conversion of arbitrary shape droplets into equivalent spheres. The lattermost error affected the calculation by an order of '$r$', as droplet information was acquired from 2D images and the pixel area of any droplet was converted into an equivalent sphere area and thereafter a sphere volume. However, qualitative calculation did indicate that insignificant evaporation happened at the bare superheated surface. The temporal and spatial evolution of the impacting droplet and its atomisation behaviour is vivid in Fig. 4.

For the nanotextured surface, a complete opposite phenomenon was observed, where complete spreading followed by liquid contact line pinning and complete evaporation could be observed (see Fig. 5). To better observe this behaviour, a top-view approach was considered to understand the heat removal. This phenomenon was similar to situations observed for Sinha-Ray and Yarin [32]. A stark dissimilarity between the work of Sinha-Ray and Yarin [32] and the current work was the surface wettability. Wherein the metal-plated surfaces offered excellent wettability to facilitate enhanced spreading followed by wicking, the PVDF coating in the current work was hydrophobic in nature. Albeit they performed similarly in terms of enhanced hydrodynamic focusing on high impact speed. As the liquid drop was focused through the porous network and spread within the architecture, the quick attainment of high temperature also led to a reduction of surface tension of water. Both phenomena led to complete wetting of the surface, which echoes the concept coined by Sahu et al. [8]. As per Lembach et al. [14], wettability driven impregnation velocity ($V$) is given as:

$$V = \left|\sigma d_{pore} cos\theta_a / 8\mu H\right|,$$

where $\theta_a$ is the advancing contact angle, $\mu$ is the dynamic viscosity, and $H$ is the layer thickness or the pore length [40].

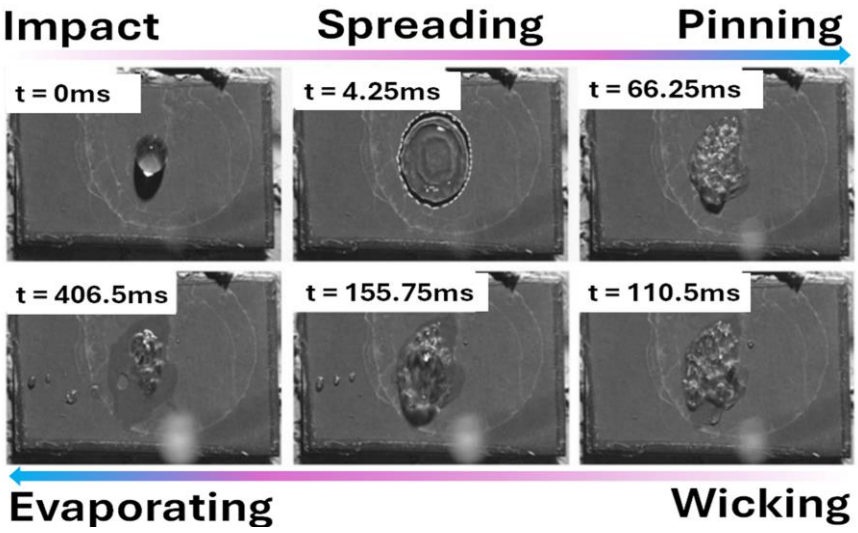


Fig. 5. Snapshots from high-speed imaging of a water droplet impacting on the superheated coated substrate; the coated surface shows impact-spread-pin-wick-evaporation behaviour.

However, this ideology works well for static cases. For the advancing contact angle greater than 90°, the above-mentioned equality does not hold. Several articles have reported penetration of liquid in hydrophobic nanofibrous membranes, like Srikar et al. [13], Sahu et al. [8], etc. For a completely non-wettable case, where $|cos\theta| \sim 1$, the above equation predicts a velocity of ~1 m/s, for the fibrous layer having $H$ ~10 μm and $d_{pore}$ ~1 μm.

During the hydrodynamic impact at one open channel, aka one pore, the focusing velocity can be approximated as, $U \approx \left(d/d_{pore}\right)V$. Considering the drop diameter ~2.8 mm, the focusing velocity ($U$) could be $>10^3$ m/s [8]. Although the liquid drop impacted several pores, and thus, dissipation of kinetic energy took place, this analysis could be safely extended to fibrous layers ~100 μm, which was a critical thickness to stop complete penetration of the impacting liquid. In our case, the kinetic energy driven hydrodynamic focusing on the thin layer ensured imbibition in the porous network and spreading of the same. This total kinetic energy dissipation and pinning of the liquid film within the nanofibres affected complete evaporation on the superheated surface.

As mentioned above, the bare surface did not affect the droplet evaporation. And hence, the bare surface did not demon-

strate any drop in surface temperature, unless complete flooding was considered. However, for an optimised condition, flooding should not be the contention in the current scope of research, as it might seem akin to jet impingement-like cooling. For the nanotextured surface, significant temperature drops were noted, and they are discussed in later sub-sections.

Using Fig. 5, we could use a simple image analysis, as described by Sinha-Ray and Yarin [32], to estimate the overall heat removal. The overall heat supply rate was 40 W, as mentioned before, whereas the loss due to convection was estimated to be 0.15 W. The wetted area on the PVDF nanofibrous coated copper substrate was obtained from top view images by first calibrating the spatial scale using the initial droplet size, which was measured gravimetrically (mass ~11.9 mg) and converted to volume (0.012 $cm^3$) using the density of water at room temperature. This radius provided the pixel-to-length conversion in ImageJ, after which the projected footprint of the spreading droplet on the coated surface was segmented frame-by-frame, and the maximum pinned wetting contour (see Fig. 5) was traced to determine the instantaneous wetted area. The maximum wetting area on the PVDF nanofibre coating was thus calculated as $A_{wetting}$ = 0.368 $cm^2$ by converting the enclosed pixel count to physical area, and an effective wetting radius $r_{eff}$ = 0.34 cm was inferred, assuming an equivalent circular footprint. With no change in initial drop volume, the heat transfer could be calculated as:

$$Q_{experiment} = (Q_{supplied} - Q_{loss})/A_{wetting},$$

suggesting a value of 108 W/$cm^2$ or 1080 kW/$m^2$.

It is to be noted that in this case, no influence of the previous droplet was present, as the drop impact happened only after complete evaporation of a previous droplet. However, since the droplet hit the surface at 125°C and eventually boiled and evaporated, another approach could be considered for measurement of the heat flux. Since the water drop, upon spreading, reached a thickness of about 0.25 mm, the thermal transient time could be estimated as $t \sim (thickness^2/\alpha_{water})$, with thermal diffusivity of water being ~1.46 ×$10^{-7}$ $m^2$/s, the evaporation time suggested a value of ~430 ms, which is similar to that in Fig. 5. Hence, the liquid layer could potentially be completely evaporated at 100°C. In this case, the total heat removal can be considered as:

$$Q_{calculation} = \frac{m[C_p(T_{saturation} - T_{impact}) + L]}{(A_{wetting} \times t_{evaporation})}.$$

With appropriate values, we can obtain $Q_{calculation}$ to be 264 W/$cm^2$ or 2640 kW/$m^2$, much higher than the visual observation and power supply. At the same time, following Ref. [32], we can find the axial heat transfer as:

$$Q_{axis} = \kappa \left[\frac{(T_\infty - T_o)}{d_{eff}}\right],$$

where $\kappa$ is the thermal conductivity of copper (~400 W/(m·K)), $T_\infty$ is the boiling temperature, $T_o$ is the wetted area temperature, and $d_{eff}$ is the effective wetting radius, which is 0.34 cm. This calculation yields a value of 294 W/$cm^2$ or 2940 kW/$m^2$. The calculation discrepancy shows that both $Q_{axis}$ and $Q_{calculation}$ consider a highly simplified version of total heat removal, whereas $Q_{experiment}$ tends to show a real value pertaining to the amount of heat flow and loss. It is to be noted that the average temperature was monitored using two thermocouples placed equidistant from the edges, and gave a near accurate value of the overall surface, as the droplet was accurately placed between two thermocouples. Neither of the theoretical calculations considered the amount of mass loss which happened during atomisation of impacting drops at film boiling conditions. It is to be noted that nearly 30% atomisation of impacting drops was observed by Park et al. [5], when the authors released a drop from a 16 cm height, nearly half the height considered here. The droplet splashing became prominent since the Ohnesorge (Oh) number was much less than 1 [$Oh = \sqrt{We}/Re$], as the viscous forces became weak, and the surface tension forces became dominant. Figure 5, bottom panels, suggested that several satellite drops could be observed on the nanotextured substrate, resulting from film boiling of the impacted drop. Such satellite drops may affect the overall calculation of heat transfer rates, since only the primary wetted area was considered here. Nevertheless, complete evaporation of the droplet occurred within a shorter time frame, and a smaller wetting area rendered the nanotextured substrate more efficient than the bare surface.

The effect of drop impact frequency was studied next to understand the steady heat transfer behaviour, especially to hasten the cooling process, yet conserving the coolant. Considering this, four such flow rates were considered: 2.85, 2.63, 2.5 and 2 s/drop (in Fig. 6, the same is indicated by s), indicating 18.9, 20.52, 21.6 and 27 ml/h. The data for bare and nanotextured surfaces are shown in Fig. 6.

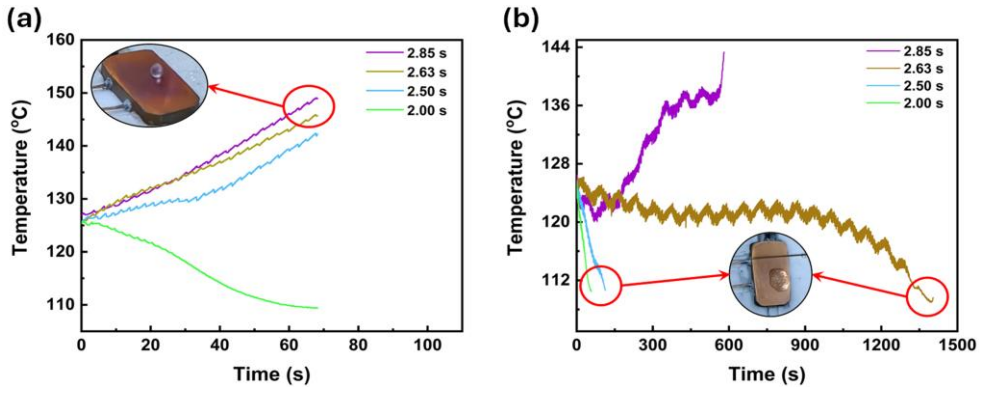


Fig. 6. Comparison of surface temperatures of (a) bare and (b) coated sample for various drop intervals, where the legends indicate the interval between two successive drops. The inset image in (a) shows the Leidenfrost effect, and in (b) shows puddle formation, respectively, for a drop interval of 2.63 s.

In the case of a bare surface, the temperature vs time behaviour was monotonous. In all cases, the upper critical temperature was kept as 140−150ºC, and upon reaching the same, the heat supply was manually stopped. During the tests, a minimum of 20 drops was allowed, and the temperature data were recorded for accurate comparison between the surfaces. For high drop intervals, the surface temperature increased nearly linearly with an upward slope (heating) of 0.33ºC and 0.28ºC per second, for 2.85 and 2.63 drops/s, respectively. This was obtained by fitting a linear relation, having an adj-$R^2$ value >0.99. For 2.5 drops/s, the slope is visibly less steep, and it showed much sluggish temperatures at the initial level. The resultant thermal increase was 0.23ºC/s (adj-$R^2$ 0.93). The higher flow rate situation, i.e., 2 drops/s, yielded a flooding condition (droplet merging with pre-existing liquid film), and eventually the surface temperature was reduced to ~110ºC, where boiling conditions did not prevail under a non-isothermal condition. From Figs. 3−4, one can notice that the impact droplet remained on the surface for nearly 2 s, which could help in liquid merging with an oncoming liquid drop, and eventually could flood the system.

The nanofibre nanotextured surface offered a favourable situation. It can be clearly seen that for the nanofibre nanotextured surface, except for a drop interval of 2.85 s, all surface coatings eventually led to surface temperature reduction to 110ºC, i.e. flooding. The drop interval time of 2.63 s led to sluggish reduction in surface temperature, eventually leading to rapid cooling and flooding after 1000 s. However, for a drop interval of 2.5 s, unlike a bare surface, the nanotextured surface showed a gradual decline of surface temperature at a rate of 0.13ºC/s. The final condition of drop interval of 2 s demonstrated the steepest cooling rate to reach 110ºC (0.24ºC/s). As per Fig. 5, the droplet evaporated within 0.4−0.5 s of drop impact, and hence, almost no interaction between previous droplets could be observed. This led to a rapid decline of the surface superheat to a significantly low value, where flooding eventually took place, in the absence of rapid evaporation.

After several trials, it was observed that for a critical drop interval of 2.7 s, relating to a flow rate of 20 ml/h, the surface temperature remained nearly constant between 122−125ºC for a 10 minute of experimentation window, when the initial test condition was 125ºC (see Fig. 7).

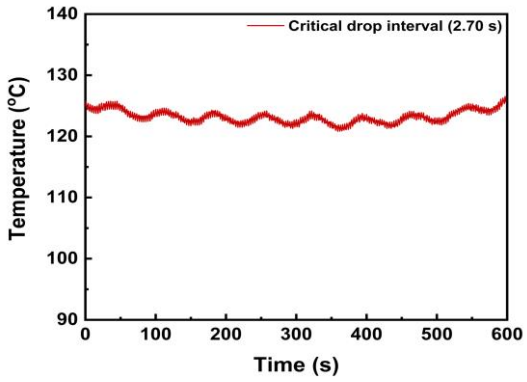


Fig. 7. Experimentally observed critical drop interval of 2.7 s, when the surface temperature varied between 122−125ºC, for an initial superheated surface temperature of 125ºC.

The repetition of the experiment yielded similar results. The term ‘critical’ here refers to a sufficient flow rate that helps remain a consistent surface temperature, neither causing a dry-out, nor resulting in any flooding on the surface. It is to be kept in mind that during the droplet frequency optimisation, two consecutive droplets never interacted. This information helps us understand the critical flow rate that allows a maximum conservation of the coolant to enhance the overall system efficiency, yet a microelectronic component performing at similar conditions. It is to be noted that this cyclic test surpassed the duration of most of the reported literature experiments, where robustness could pose a concern. One of the longest test durations of drop impact heat transfer on a polymeric fibre mediated surface at a constant elevated temperature was 180 s, as per Ref. [33]. Figure 7 showed that for 600 s, the architecture remained the same as the heating-cooling cycles were identical.

To evaluate the long-term durability of the nanotextured sample, cyclic testing was conducted over an extended period. Representative cyclic testing data are shown in Fig. 8. In this case, the upper limit of 130ºC was considered as the baseline of the high-power IC degradation temperature, and can be called an upper critical limit, whereas 110ºC was considered its operating temperature. It was already observed that for a drop interval of 2.5 s, the superheated surface temperature reduction followed a steady optimised decline. Hence, in this case, the same drop interval was chosen. However, in this case, puddle formation was allowed, and temperature drop was followed. The temperature drop was allowed till 80ºC, where puddle formation was seen at 110ºC. Once the temperature reached 80ºC, the coolant supply was stopped till the temperature reached 125ºC again. During the whole process, the heat supply was maintained. This was analogous to the continuous operation of an integrated circuit (IC) at the same power.

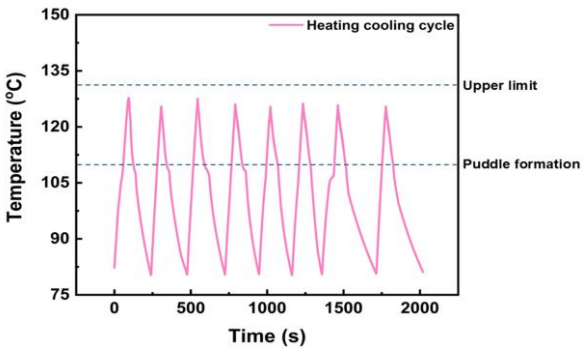


Fig. 8. Cyclic heating-cooling of a coated copper sample at a drop interval of 2.5 s – a representative data set of the entire cyclic heating-cooling.

In industry practices, high-power ICs are often tested against 125ºC and in such consideration, the test method mentioned here may provide a positive exposure to the robustness of the coating. The heating-cooling cycles for the entire time duration were identical. This truly demonstrates the excellent adherence of the nanofibrous coating and displays the robustness of the porous architecture despite the demanding applications. At the same time, this test demonstrated that for a 2.5 s interval per drop,

a significant amount of coolant can be preserved. A single cycle of 80ºC−125ºC−80ºC required 240 s, out of which about 95 s was required for the substrate to reach 125ºC from 80ºC. This also meant that during the experiment, 0.57 ml of water was preserved during the heating operation, whereas 0.87 ml of water was utilised during the entire cooling process. This signifies that during the entire process of heating and cooling, a 39.6% coolant volume was preserved, in comparison to continuous cooling.

## 5. Conclusions

The present study aims to investigate the effect of polymer nanofibrous nanotexture on superheated surface exposed to drop-impact cooling, especially related to microelectronics thermal management. A novel coating technique was employed, called supersonic solution blowing, to deposit nanofibres of diameter <250 nm on a copper substrate mimicking a heat sink for high-power microelectronics. The deposited layer exhibited a thin adherent milky appearance. The nanofibrous architecture retained its structure after water drop impact with a high Weber number. Unlike the bare copper surface, where impacting liquid drop bouncing and a Leidenfrost like escape could be observed, here, a complete pinning of liquid drops, along with wetting and wicking through porous architecture was evident. Despite the layer being hydrophobic, strong hydrodynamic focusing allowed liquid imbibition upon impact. The nanotexture surface could potentially remove as high as a ~1080 kW/m$^2$ heat flux. This high value opens a great scope to explore spray cooling like applications on soft polymeric materials.

Further studies focusing on interval/drop rate optimisation established a drop interval of 2.5 s to be the most effective one in controlling the heating of microelectronics. A long cyclic testing of heating and cooling demonstrated the robustness of such nanotexturing without any sign of delamination. Such a test also showed that instead of continuous cooling, a periodic supply of coolant can be equally effective in preserving the coolant.

## Acknowledgements

The authors would like to thank the Indian Institute of Technology Delhi (IIT Delhi) for its research support, including assistance from the Central Research Facility and the Central Workshop of IIT Delhi. RP appreciates the financial support provided by the Ministry of Education, Government of India. PKS and SS-R acknowledge the financial assistance from National Technical Textile Mission (NTTM), under the Ministry of Textiles, Government of India (project code RP04675). This work was presented at ICRAME 2025.

## References

[1] Kumar, H., & Sehga, S.S. (2013). Study of fluid flow and heat transfer through mini-channel heat sink. *Asian Journal of Engineering and Applied Technology*, 2(2), 25–28. doi: 10.51983/ajeat-2013.2.2.686

[2] Slattery, O.F., Kelly, G., & Greer, J. (2000). Thermal and mechanical problems in microelectronics. In *Benefiting from Thermal and Mechanical Simulation in Micro-Electronics* (pp. 17–26). Springer, Boston. doi: 10.1007/978-1-4757-3159-0_2

[3] BW Online Bureau. (2024). *India's Electronics Manufacturing Likely To Double In Next 5 Yrs: Report* - BW BusinessWorld. https://www.businessworld.in/article/indias-electronics-manufacturing-likely-to-double-in-next-5-yrs-report-529982 [accessed 30 Dec. 2025].

[4] Alahmad, M., & Abd El-Aleem, F. (2003). Heat transfer challenges in semiconductors processing and the applications of heat pipes for efficient heat removal. *Journal of King Saud University-Engineering Sciences*, 15(1), 141–154. doi: 10.1016/S1018-3639(18)30767-0

[5] Park, C., Seol, J., Aldalbahi, A., Rahaman, M., Yarin, A.L., & Yoon, S.S. (2023). Drop impact phenomena and spray cooling on hot nanotextured surfaces of various architectures and dynamic wettability. *Physics of Fluids*, 35(2), 027126. doi: 10.1063/5.0139960

[6] Jun, S., Sinha-Ray, S., & Yarin, A.L. (2013). Pool boiling on nano-textured surfaces. *International Journal of Heat and Mass Transfer*, 62(1), 99–111. doi: 10.1016/j.ijheatmasstransfer.2013.02.046.

[7] Kareem, R., Panicker, M.R.R., & Namboothiri, V.N.N. (2023). A review on immersion cooling of electronic systems. *AIP Conference Proceedings*, 2863, 020007. doi: 10.1063/5.0155307

[8] Sahu, R.P., Sinha-Ray, S., Yarin, A.L., & Pourdeyhimi, B. (2012). Drop impacts on electrospun nanofiber membranes. *Soft Matter*, 8(14), 3957–3970. doi: 10.1039/C2SM06744G

[9] Yan, Z., Jin, M., Li, Z., Zhou, G., & Shui, L. (2019). Droplet-based microfluidic thermal management methods for high performance electronic devices. *Micromachines*, 10(2), 89. doi: 10.3390/mi10020089

[10] Don Houk (2020). *What You Should Know About Computers and Heat.* Next7 IT. https://www.next7it.com/insights/know-about-computers-heat/ [accessed 30 Dec. 2025].

[11] Kim, S., Wang, T., Zhang, L., & Jiang, Y. (2020). Droplet impacting dynamics on wettable, rough and slippery oil-infuse surfaces. *Journal of Mechanical Science and Technology*, 34, 219−228. doi: 10.1007/s12206-019-1223-z

[12] Vaikuntanathan, V., & Sivakumar, D. (2012). Directional motion of impacting drops on dual-textured surfaces. *Physical Review E—Statistical, Nonlinear, and Soft Matter Physics*, 86(3), 36315. doi: 10.1103/PhysRevE.86.036315

[13] Srikar, R., Gambaryan-Roisman, T., Steffes, C., Stephan, P., Tropea, C., & Yarin, A.L. (2009). Nanofiber coating of surfaces for intensification of drop or spray impact cooling. *International Journal of Heat and Mass Transfer*, 52(25–26), 5814–5826. doi: 10.1016/ j.ijheatmasstransfer.2009.07.021

[14] Lembach, A.N., Tan, H.B., Roisman, I.V., Gambaryan-Roisman, T., Zhang, Y., Tropea, C., & Yarin, A.L. (2010). Drop impact, spreading, splashing, and penetration into electrospun nanofiber mats. *Langmuir*, 26(12), 9516–9523. doi:10.1021/la100031d.

[15] Reneker, D.H., & Yarin, A.L. (2008). Electrospinning jets and polymer nanofibers. *Polymers with Aligned Carbon Nanotubes: Active Composite Materials*, 49(10), 2387–2425. doi: 10.1016/j.polymer.2008.02.002.

[16] Marengo, M., Antonini, C., Roisman, I.V, & Tropea, C. (2011). Drop collisions with simple and complex surfaces. *Current Opinion in Colloid & Interface Science*, 16(4), 292–302. doi: 10.1016/j.cocis.2011.06.009

[17] Lee, M., Chang, Y.S., & Kim, H.-Y. (2010). Drop impact on microwetting patterned surfaces. *Physics of Fluids*, 22(7), 072101. doi: 10.1063/1.3460353

[18] Li, H., Fang, W., Zhao, Z., Li, A., Li, Z., Li, M., Li, Q., Feng, X., & Song, Y. (2020). Droplet precise self-splitting on patterned adhesive surfaces for simultaneous multidetection. *Angewandte*

*Chemie International Edition*, 59(26), 10535–10539. doi: 10.1002/anie.202003839

[19] Zhao, Y.-P., & Yuan, Q. (2015). Statics and dynamics of electrowetting on pillar-arrayed surfaces at the nanoscale. *Nanoscale*, 7(6), 2561–2567. doi: 10.1039/C4NR06759B

[20] Xiong, Y., Huang, H., & Lu, X.-Y. (2020). Numerical study of droplet impact on a flexible substrate. *Physical Review E*, 101(5), 53107. doi: 10.1103/PhysRevE.101.053107

[21] Liu, X., Zhang, X., & Min, J. (2019). Maximum spreading of droplets impacting spherical surfaces. *Physics of Fluids*, 31(9), 092102. doi: 10.1063/1.5117278

[22] Teja, T.C., Reddy, N.V.D., & Santra, S. (2025). Spreading and breakup dynamics of successive droplets impacting a curved surface. *Colloids and Surfaces A: Physicochemical and Engineering Aspects*, 717, 136794. doi: 10.1016/j.colsurfa.2025.136794

[23] Santra, S., Mandal, S., & Chakraborty, S. (2021). Phase-field modeling of multicomponent and multiphase flows in microfluidic systems: A review. *International Journal of Numerical Methods for Heat and Fluid Flow*, 31(10), 3089–3131. doi: 10.1108/HFF-01-2020-0001

[24] Fu, Z., Jin, H., Yao, G., & Wen, D. (2024). Droplet impact simulation with Cahn–Hilliard phase field method coupling Navier-slip boundary and dynamic contact angle model. *Physics of Fluids*, 36(4), 042115. doi: 10.1063/5.0202604

[25] Kim, H., Truong, B., Buongiorno, J., & Hu, L.-W. (2011). On the effect of surface roughness height, wettability, and nanoporosity on Leidenfrost phenomena. *Applied Physics Letters*, 98(8), 083121. doi: 10.1063/1.3560060

[26] Kwon, H., Bird, J.C., & Varanasi, K.K. (2013). Increasing Leidenfrost point using micro-nano hierarchical surface structures. *Applied Physics Letters*, 103(20), 201601. doi: 10.1063/1.4828673

[27] Geraldi, N.R., McHale, G., Xu, B.B., Wells, G.G., Dodd, L.E., Wood, D., & Newton, M.I. (2016). Leidenfrost transition temperature for stainless steel meshes. *Materials Letters*, 176, 205–208. doi: 10.1016/j.matlet.2016.04.124

[28] Takata, Y., Hidaka, S., Cao, J.M., Nakamura, T., Yamamoto, H., Masuda, M., & Ito, T. (2005). Effect of surface wettability on boiling and evaporation. *Energy*, 30(2–4), 209–220. doi: 10.1016/j.energy.2004.05.004

[29] Weickgenannt, C.M., Zhang, Y., Lembach, A.N., Roisman, I.V., Gambaryan-Roisman, T., Yarin, A.L., & Tropea, C. (2011). Non-isothermal drop impact and evaporation on polymer nanofiber mats. *Physical Review E - Statistical, Nonlinear, and Soft Matter Physics*, 83(3), 1–13. doi: 10.1103/PhysRevE.83.036305

[30] Sinha-Ray, S., Zhang, Y., & Yarin, A.L. (2011). Thorny devil nanotextured fibers: The way to cooling rates on the order of 1 kW/cm$^2$. *Langmuir*, 27(1), 215–226. doi: 10.1021/la104024t

[31] Sahu, R.P., Sett, S., Yarin, A.L., & Pourdeyhimi, B. (2015). Impact of aqueous suspension drops onto non-wettable porous membranes: Hydrodynamic focusing and penetration of nanoparticles. *Colloids and Surfaces A: Physicochemical and Engineering Aspects*, 467, 31–45. doi: 10.1016/j.colsurfa.2014.11.023

[32] Sinha-Ray, S., & Yarin, A.L. (2014). Drop impact cooling enhancement on nano-textured surfaces. Part I: Theory and results of the ground (1 g) experiments. *International Journal of Heat and Mass Transfer*, 70, 1095–1106. doi: 10.1016/j.ijheatmasstransfer.2013.11.007

[33] Sinha-Ray, S., Sinha-Ray, S., Yarin, A.L., Weickgenannt, C.M., Emmert, J., & Tropea, C. (2014). Drop impact cooling enhancement on nano-textured surfaces. Part II: Results of the parabolic flight experiments [zero gravity (0g) and supergravity (1.8g)]. *International Journal of Heat and Mass Transfer*, 70, 1107–1114. doi: 10.1016/j.ijheatmasstransfer.2013.11.008

[34] Thakur, S.S., Chandel, S.S., Kakoria, A., & Sinha-Ray, S. (2022). Enhancement in pool boiling heat transfer of ethanol and nanofluid on novel supersonic nanoblown nanofiber textured surface. *Experimental Heat Transfer*, 35(4), 516–532. doi: 10.1080/08916152.2021.1919243

[35] Pippal, R., Shukla, P.K., & Sinha-Ray, S. (2025). Enhancing boiling heat transfer on an ultrafine nanofibrous coated superheated surface using ethanol/SWCNT Nanofluid. *Thermal Science and Engineering Progress*, 65, 103876. doi: 10.1016/j.tsep.2025.103876

[36] Sahu, R.P., Sinha-Ray, S., Sinha-Ray, S., & Yarin, A.L. (2016). Pool boiling of Novec 7300 and self-rewetting fluids on electrically-assisted supersonically solution-blown, copper-plated nanofibers. *International Journal of Heat and Mass Transfer*, 95, 83–93. doi: 10.1016/j.ijheatmasstransfer.2015.11.094

[37] Sinha-Ray, S., Zhang, W., Stoltz, B., Sahu, R.P., Sinha-Ray, S., & Yarin, A.L. (2017). Swing-like pool boiling on nano-textured surfaces for microgravity applications related to cooling of high-power microelectronics. *npj Microgravity*, 3, 9. doi: 10.1038/s41526-017-0014-z

[38] Sinha-Ray, S., Zhang, W., Sahu, R.P., Sinha-Ray, S., & Yarin, A.L. (2017). Pool boiling of Novec 7300 and DI water on nano-textured heater covered with supersonically-blown or electrospun polymer nanofibers. *International Journal of Heat and Mass Transfer*, 106, 482–490. doi: 10.1016/j.ijheatmasstransfer.2016.08.101

[39] Khooshehchin, M., Mohammadidoust, A., & Ghotbinasab, S. (2020). An optimization study on heat transfer of pool boiling exposed ultrasonic waves and particles addition. *International Communications in Heat and Mass Transfer*, 114, 104558. doi: 10.1016/j.icheatmasstransfer.2020.104558

[40] Washburn, E.W. (1921). Note on a method of determining the distribution of pore sizes in a porous material. *Proceedings of the National Academy of Sciences*, 7(4), 115–116. doi: 10.1073/pnas.7.4.115